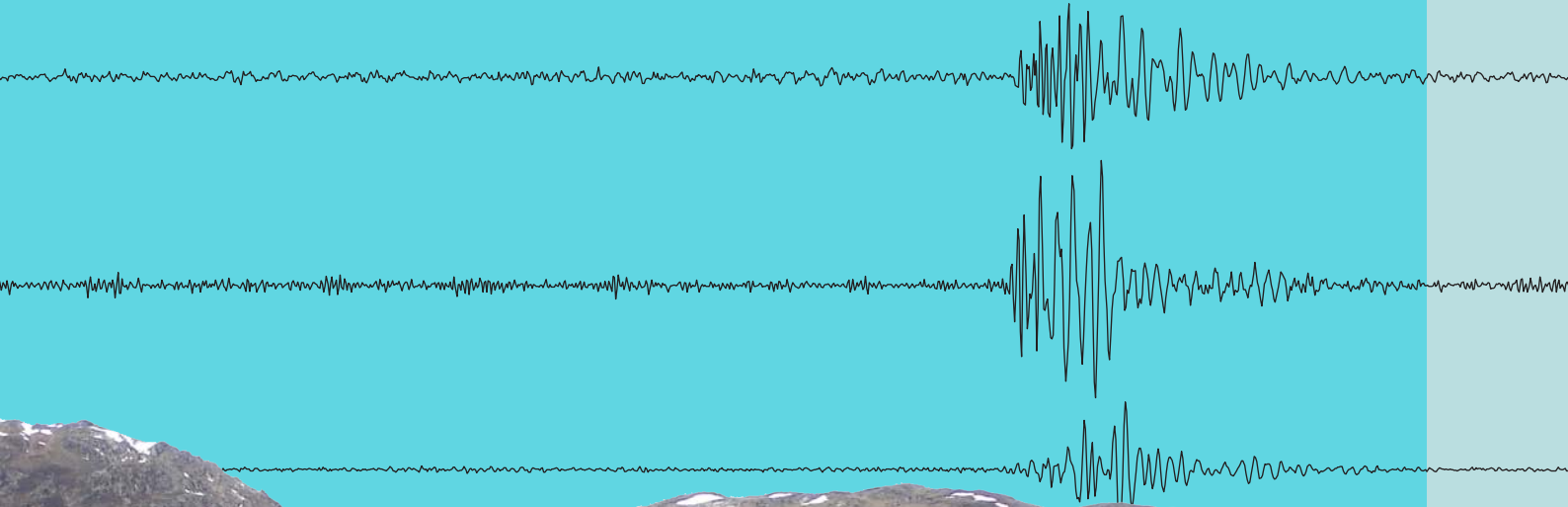


# Hazard Estimation of Deep Seated Mass Movements by Microseismic Monitoring

ISDR20 - Final Report

Stefan Mertl, Ewald Brückl



**OAW**  
Austrian Academy  
of Sciences

# Hazard Estimation of Deep Seated Mass Movements by Microseismic Monitoring

## ISDR20 Final Report 2004 - 2008

Stefan Mertl, Ewald Brückl

**Principal Investigator:** Ewald Brückl

**Working Group:**

Daniel Binder, Helmut Hausmann, Stefan Mertl

### CONTENTS

1	Introduction	1
2	Monitoring Networks	2
2.1	Pilot study Gradenbach – broadband monitoring station	2
2.2	Short-time monitoring	2
2.3	Permanent monitoring network Gradenbach	3
3	Data Handling	4
3.1	Data Collection	4
3.2	Data Storage and data conversion	4
4	Data Processing	4
4.1	Overview	4
4.2	Event detection	4
5	Interpretation	7
5.1	Event classification	7
5.2	Event localization	9
6	Results	9
6.1	Overview	9
6.2	Gradenbach	9
6.3	Steinlehen rock slide	11
7	Discussion	12
8	References	13
	Appendix	14
	A. Seismon – Data handling and processing Software	14
	B. Temporal distribution of events	16



Institute of Geodesy and Geophysics, Vienna University of Technology  
Vienna, September 2008

Online ISBN: 978-3-7001-6533-0  
doi: 10.1553/ISDR-20

*Cover: Mass-movement Gradenbach and seismograms of a microseismic event.*

# 1 Introduction

The task of the ISDR-20 (TUW - Vienna University of Technology) and ISDR-21 (TUG – Graz University of Technology) projects is the integration of geodetic and geophysical monitoring into a uniform surveillance system for deep-seated mass movements. The combination of continuous GPS measurements, high resolution strain meter observations, and a local seismic monitoring network should lead into an Integrated Monitoring System (IMoS). Seismic monitoring yields information on fracture and stick-slip phenomena caused by the mass movement, the strain meter will monitor local strain changes, and GPS measurements result in the medium to long term trend of surface displacements. Another aspect of GPS and broad band seismic monitoring is the coverage of the whole spectrum of movement, which ranges from quasi-continuous displacement via stick-slip to critical fracture. The combination of the two methods offers the opportunity to monitor displacements over a very broad frequency band from periods of seismic waves ( $\sim 1/100$  second) via short-time oscillation (minutes to hours) to long-time trends (several years). Interpretation of IMoS data will be based on structural models of the mass movements, developed by earlier projects within IDNDR and ISDR.

The development of IMoS is in tight cooperation with Prof. F.K. Brunner, TUG. The test site is the well-investigated deep-seated mass movement Gradenbach. Another seismic monitoring campaign has been accomplished at Niedergallmig/Matekopf (Tirol) in cooperation with alpS (project A.2.4). This cooperation includes the sharing of seismic equipment and scientific data. For the seismic monitoring tasks, cooperation with Dr. M. Joswig, Institute of Geophysics, University of Stuttgart, has already been established.

E. Brückl had the opportunity of a two weeks stay at Niigata University, Japan, and to participate also INTERPRAEVENT 2006 in September 2006. A paper covering the essential results of seismic monitoring within ISDR-20 was presented (Brückl and Mertl, 2006) and a special report covering experiences and new ideas developed during this visit was already sent to ÖAW.

In July 2007 E. Brückl was invited to present a paper at the 11th congress of the International Society for Rock Mechanics at Lisbon, Portugal. The paper describes the current progress in event detection and localization of microseismic events on deep-seated mass movements gained within the ISDR-20 project (Mertl and Brückl, 2007).

## 2 Monitoring Networks

### 2.1 Pilot study Gradenbach – broadband monitoring station

On the 7<sup>th</sup> of September 2004 one Guralp CMG-6TD digital broadband seismometer has been installed at the station MA (see Figure 1). At this station a permanent GPS monitoring station is run by the Graz University of Technology (TUG). The broadband station was intended to give an overview of the seismic activity and the data quality that could be expected at Gradenbach. Furthermore it provided valuable insights in the system design and the data handling process to develop an all-season monitoring station.

### 2.2 Short-time monitoring

#### 2.2.1 Overview

Before and parallel to the permanent monitoring at Gradenbach (GB), several short-time monitoring projects have been accomplished at different mass-movements (see Table 1). The aim of these monitoring projects was to collect information of seismic events recorded at various mass-movements and the search for possible similarities between events recorded at the individual monitoring sites. Moreover the knowledge gained within these monitoring projects supported the development of equipment suitable for permanent seismic monitoring.

Date	Project	Location	Stations
14.06.2005 - 23.06.2005	GB200506	Gradenbach	6
14.09.2005 - 22.09.2005	HA200509	Hochmais / Atemskopf	5
08.06.2006 - 27.07.2006	NG200606	Niedergallmigg / Matekopf	13
03.07.2007 - 12.07.2007	SL200707	Steinlehen	10

Table 1: Overview of short-time monitoring projects accomplished within ISDR20.

#### 2.2.2 GB200506 (Gradenbach)

Additional to the broadband station installed for the pilot study at station MA, five 3-component 4.5 Hz stations have been deployed from 14.06.2005 to 23.06.2005 at Gradenbach (see Figure 1). Each station consisted of 3 Reftek 125-01 (Texan) units and a 4.5Hz 3-component geophone. The Texans were placed in a robust, waterproof case and powered by a 12V battery.

To enable a long recording period, the Texans were equipped with 256 MB of internal memory and the power supply has been modified to support an external 12V battery. With these modifications, the Texans could record up to 9.5 days at a sampling rate of 100 samples per second (sps).

#### 2.2.3 HA200509 (Hochmais / Atemskopf)

In September 2005, from 14.9. to 22.9., five 3-component stations have been installed at Hochmais / Atemskopf (see Figure 2). The equipment used was similar to the one used in GB200506. The data has been sampled with 100 sps.

#### 2.2.4 NG200606 (Niedergallmigg)

In cooperation with alpS (project A.2.4) the monitoring project NG200606 has been accomplished at Niedergallmigg / Matekopf (Tirol) in June-July 2006. Thirteen stations have been deployed on the mass-movement (see Figure 3). Three different recording systems have been used (see Table 2) and provided an overview of the usability of each system for a permanent installation.

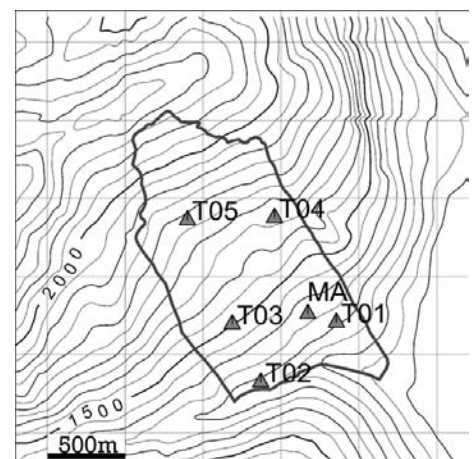


Figure 1: Seismic monitoring network of project GB200506

**2.2.5 SL200707 (Steinlehen, Gries im Sellrain)**

In June/July 2003 acceleration of a slab at Steinlehen induced a series of rock fall events. After this acceleration, the slope velocity continuously decreased until spring 2004, when the slide re-accelerated again followed by another period of stabilization (Zangerl *et al.*, 2007).

In cooperation with alpS, a seismic monitoring network has been installed from 03.07.2007 to 12.07.2007 at the mass-movement Gries–Steinlehen. The aim of this monitoring task was the investigation of the seismic activity of a highly active slab (HAS, see Figure 4). The network consisted of ten stations, each equipped with one ELGI-DAS digitizer and datalogger, a 1Hz three-component geophone and a 12V battery as power supply. The data was recorded continuously with 200 sps.

Station	Recorder	Geophone / Seismometer
3, 4, 5, 6, 7	Reftek 130-1	GS-11D 4.5Hz 3-component
1	Guralp 6TD	Guralp 6TD 30s - 1Hz 3-component
2, 8, 9, 10	Reftek Texan	GS-11D 4.5Hz 3-component
11, 12, 13	Reftek Texan	GS-11D 4.5Hz vertical

Table 2: Seismic equipment used for monitoring project NG200606.

**2.3 Permanent monitoring network Gradenbach**

The 31st of August 2006 two monitoring stations have been installed at Gradenbach. These stations have been extended to a five stations monitoring network at the beginning of November 2006. In May 2007 a sixth station has been added to the seismic monitoring network (see Figure 5). Also in May 2007, the Guralp broadband seismometer has been moved from station GB01 to GB04 where the team of the TU Graz has installed a tree-axial strainmeter in order to realize IMoS. All stations have a solar power supply and a lightning protection. The sensor is buried in a depth of at least 60cm and the electric equipment is stored in a metal box for weather protection.

The data is recorded in continuous mode without any event trigger used. Data is recorded at 100 sps during winter and 200 sps during summer time, except station GB04 which supports 100 sps as the maximum sampling rate. From November to March, the stations are not safely accessible and the reduction of the sampling rate to 100 sps prevents data loss caused by data storage overflow. This is valid for all stations except GB04, for which the fixed storage capacity of 4 GB prevents a continuous data recording for more than approx. 80 days, so data loss during winter at GB04 has to be expected.

The maximum possible recording duration for the used equipment configuration can't be determined exactly, because it depends on the compression rate and the noise level at the station. As a point of reference, a Reftek130-1 records 116 days at 200sps and 240 days at 100sps.

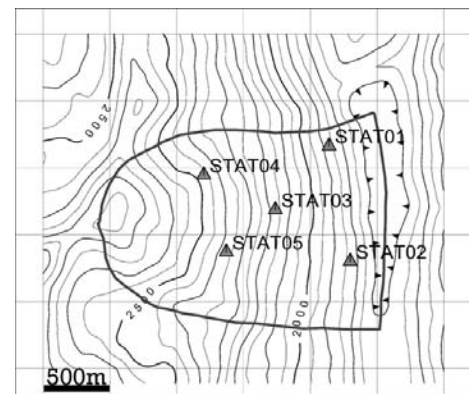


Figure 2: Monitoring network of project HA200509.

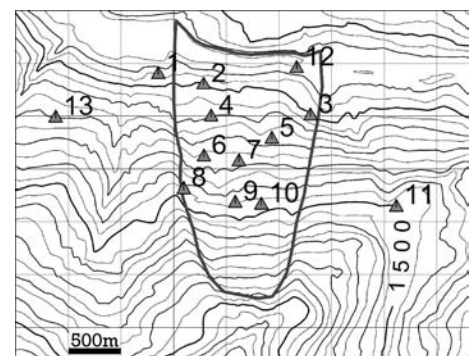


Figure 3: Monitoring network of project NG200606.

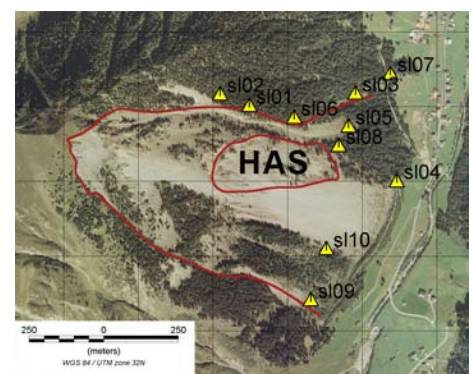


Figure 4: Monitoring network of project SL200707. Orthophoto: "Land Tirol – tiris"

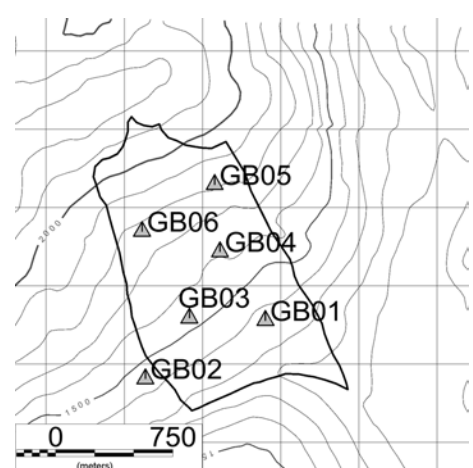


Figure 5: Monitoring network of the permanent project at Gradenbach.

## 3 Data Handling

### 3.1 Data Collection

The data collection procedure is explained based on the monitoring equipment used at GB. The data is stored internally on flash memory by the digitizer units. Each Reftek130-01 unit at the permanent monitoring network Gradenbach is equipped with two 4GB CF cards. The data can be collected on site by swapping the CF cards. The data is copied to a harddisk after collecting the CF cards from all stations of the monitoring network. The Guralp 6TD has 4GB of internal flash memory which can be downloaded on site using an external harddisk and a firewire connection.

The data is collected approximately every 3 months. During winter, this interval can not always be sustained. Therefore a data loss at station GB04 might occur.

### 3.2 Data Storage and data conversion

After collecting the data from the monitoring network, it is stored on a harddisk and a backup system. The Reftek raw data and the Guralp raw data is converted to miniSeed file format for further processing. These conversion steps are done using Seismon (see Appendix A) as a frontend for the conversion programs provided by the equipment manufacturer.

## 4 Data Processing

### 4.1 Overview

Processing of the micro-seismic network data requires a frequent and ongoing development of new methods and algorithms. Most commercial (e.g. ANTELOPE) and free (SEISAN (Havskov and Ottemöller, 1999), MATSEIS (Hart *et al.*, 2005)) software products are configured for the use within standard seismological projects and adaption of existing code provides not as much flexibility as needed. Therefore the development of Seismon was started with the ISDR20 project (see Appendix A). Seismon provides all data handling and processing steps to analyze data of small scale seismic networks. Its modular coding approach enables the quick integration of new code and therefore makes Seismon a flexible tool for scientific seismic data processing. It is already in use within several projects at the Institute of Geodesy and Geophysics (Alp2002, ALPASS, Permafrost in Austria, Tunnel Seismic while Drilling) and it has been used within two diploma thesis attended to the Institute of Geodesy and Geophysics.

### 4.2 Event detection

The high background noise level caused by farming-, traffic- or environmental noise makes the detection and identification of micro-earthquakes excited by the mass movement a crucial task.

When looking at a spectrogram or a sonogram (Joswig, 1994, Joswig, 1990) of a seismic trace, an expert is able to immediately identify abnormal patterns in the seismogram and to distinguish between seismic events and noise. Humans treat these spectrograms as images and classify the patterns according to their shape and location in the spectrogram.

Therefore, the approach of accounting and treating the spectrogram as an image stands to reason. Image processing techniques provide valuable tools to extract patterns from spectrogram images and to describe their shape. A seeded region growing algorithm is used to segment the spectrogram images and cluster analysis links the extracted patterns found on different stations of the monitoring network to combined events.

#### 4.2.1 Pattern extraction

The extraction of demonstrative patterns in the spectrogram is the first step in the event detection process. The pattern extraction does not validate the shapes. It searches for patterns which silhouette against the background noise and therefore may be of special interest.

For a given time window (e.g. 300 seconds), the spectrogram is calculated using a short time Fourier transform. Background noise removal and an intensity transformation are applied to enhance the weak signal content (Gonzalez and Woods, 2002).

The extraction of the patterns from the spectrogram is done by image segmentation using a seeded region-growing algorithm (Gonzalez and Woods, 2002, Mehnert and Jackway, 1997). The main steps of the pattern extraction process are shown in Figure 6. First, the spectrogram is calculated. For this spectrogram, the seed points are computed by thresholding the spectrogram image. These seed points and a blurred version of the spectrogram are the input of the region-growing algorithm. The result is a matrix containing the labeled patterns.

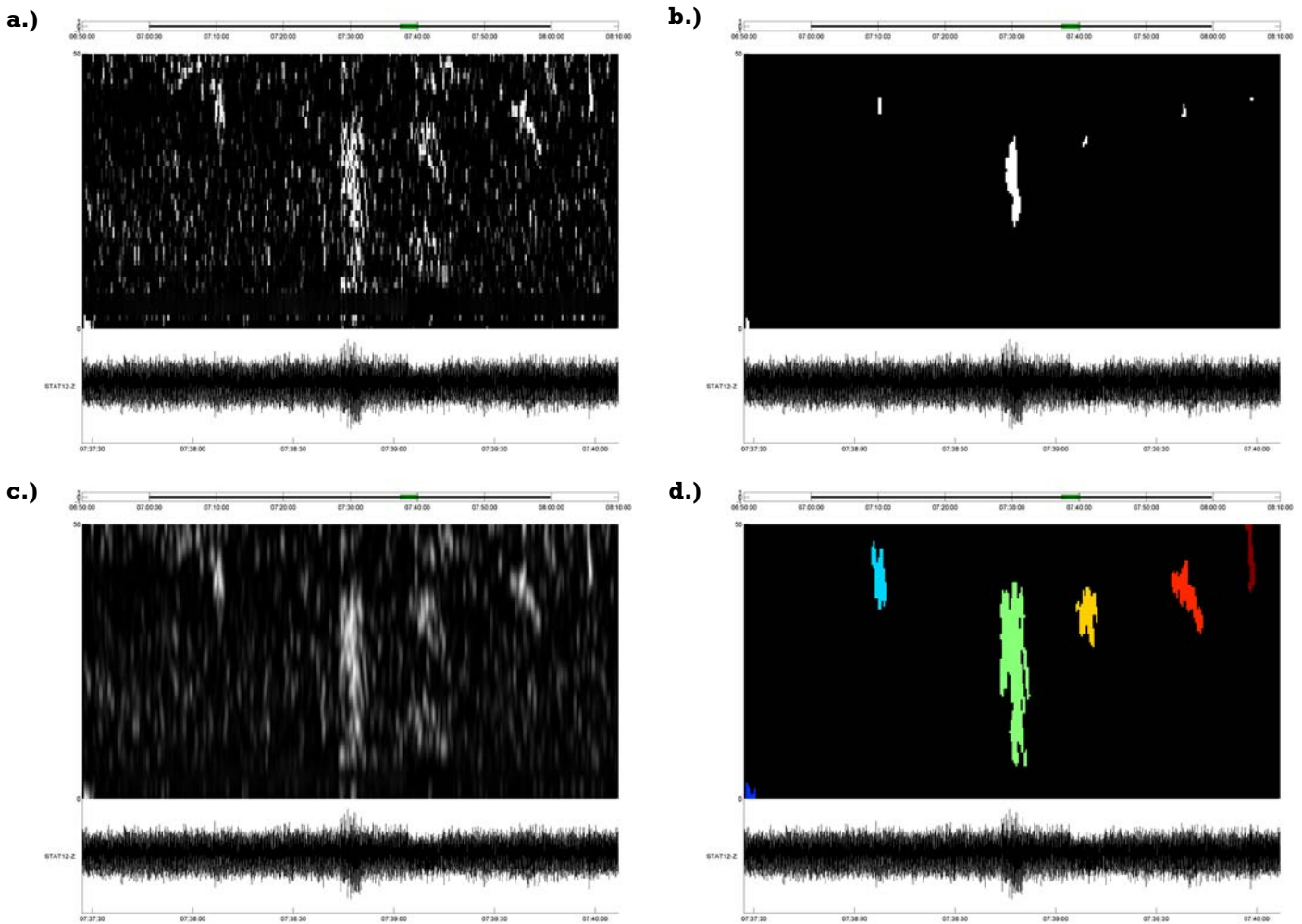


Figure 6: a) The calculated spectrogram of the seismic trace. The random granular noise is caused by the background noise removal. b) The seed points are created by thresholding the spectrogram image (a). To eliminate the granular noise, the created seed point image is filtered with a 2D median filter. c) A blurred (low pass filtered) version of the spectrogram image (a) is calculated. This blurred spectrogram and the seed points are the input of the region growing algorithm. The usage of a blurred spectrogram image causes the region growing algorithm to close small gaps in the spectrogram image patterns. d) The result of the region growing algorithm is a binary image (or matrix) with 1 indicating a pattern and 0 indicating no pattern. The final process links neighboring pattern pixels and labels them with a number, which makes it possible to distinguish between the individual patterns.

#### 4.2.2 Cluster analysis

The pattern extraction described above is a single trace process with no classification of the found patterns. The information contained in the multiple stations of the monitoring network is used in the cluster analysis step to link the individual patterns to combined events and to assign a quality attribute.

For each of the patterns, characteristic features are calculated (first-break, bandwidth, centroid). According to these features, the patterns are clustered. Each cluster is treated as an event. The number of traces on which a pattern contributing to the event is found gives the quality attribute.

First, the patterns are clustered according to their first-break, which is the most important feature of the three mentioned above. Next, each of the clusters is clustered again according to the bandwidth and the centroid of the patterns. This splits events, that consist of seismic noise patterns occasionally happening at the same time, but which have a different shape in the spectrogram. The result of these two cluster steps is a list of events with the amount of stations on which the event has been recorded as a quality attribute. The clustering of the events and the classification with the quality attribute helps to reduce the events that have to be checked by a human operator. An example of the clustering of an event covered with seismic noise events is given in Figure 7. A low frequent signal (most likely a global earthquake) is recorded on 5 stations and clustered to an event (yellow pattern) with a high quality attribute. The other patterns are identified as single station events and will therefore get a low quality attribute.

### 4.2.3 Automation

The pattern extraction and cluster analysis is implemented as a package in the Seismon software. The event detection can be run automated and the extracted patterns and detected events are stored in a database for later inspection. A database frontend makes it easy to manage, visualize and classify the detected events. See Appendix A for more details on the Seismon software.

The automation includes the extraction of patterns which stand out against the background noise. But no interpretation of the extracted signals is done up to this point. With the current state of knowledge about micro-seismic events on deep-seated mass-movements we would not recommend an automated interpretation of recorded signals. Automated interpretation always requires some sort of previous knowledge about the signals which should be interpreted. The interpretation of signal characteristics which occur for the first time and for which no previous knowledge is available is a crucial task. In such situations, the intuition of a human beats the processing power of a computer.

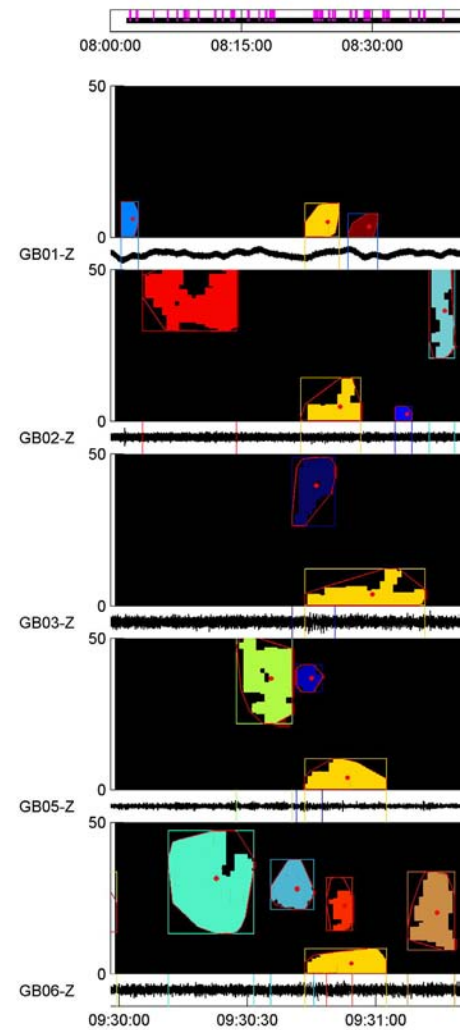


Figure 7: Example of the clustering of a local earthquake. Patterns associated to a combined event have the same color. The five yellow patterns have been linked together to a combined event with a high quality attribute (event is present at five stations).

## 5 Interpretation

### 5.1 Event classification

The identification of events is done manually by a human operator (S. Merti). Each of the automatically detected events is inspected visually and compared to the earthquake bulletin of the *Central Institute for Meteorology and Geodynamics (ZAMG)*. This helps to eliminate local, regional and global earthquakes from the detected events.

Based on waveform, frequency content and spectrogram shape, the events are divided into several classes. All events which can't be assigned to a known seismic event not related to the mass-movement are labelled as *candidates*. For candidate events with similar waveform and spectrogram occurring frequently throughout the observation period, event types have been introduced (Table 3).

All candidate events are furthermore compared with the recordings on observatory stations nearby the monitoring network. This enables the elimination of candidates, which are local earthquakes, but not listed in the earthquake bulletin. The waveform data of the nearby observatory stations is downloaded from the *Observatories and Research Facilities for European Seismology (ORFEUS)* using ftp.

Type	Description
A	Short single event. Duration of ca. 2 seconds. The event is isolated in time with no precursor or successor. The frequency content varies but most often shows high frequent content (> 25Hz).
B	Event with a long duration (10s and more). Usually there is no clear first break visible. The frequency content is between 1 and 25 Hz.
C	Event with the signature of a local earthquake. The duration is between 4 and 15 seconds. The event is characterized by a sharp onset with high frequency content and a later second maximum with a lower frequency content representing the s-waves. There is no coincident earthquake listed in the bulletin. The major frequency content lies between 5 and 20 Hz.
D	Low frequency event. This event is characterized by a maximum in the area between 3Hz and 5Hz. The waveform is quite monochromatic. The duration varies between 5 and 15 seconds.
E	Event with long travel-time differences between each station. The event has a sharp onset and high frequency content (10 to >50 Hz). Most likely an air blast.
F	Event with multiple sub events following each other. The events occur in swarms and show high frequency onsets and low frequent, monochromatic successors. The duration of the event varies between 4 and 20 seconds and it's main frequency content is concentrated between 5 and 25 Hz.
Z	Undefined event that fits in no other type or is a mixture of other types.

Table 3: Event types of candidate events.

### 5.1.1 Candidate Event type examples

Figure 8 gives an overview of the candidate event types. The division into the event types is based on waveform and spectrogram shape. Type Z is not shown because a distinct example representing all events of this type can't be given.

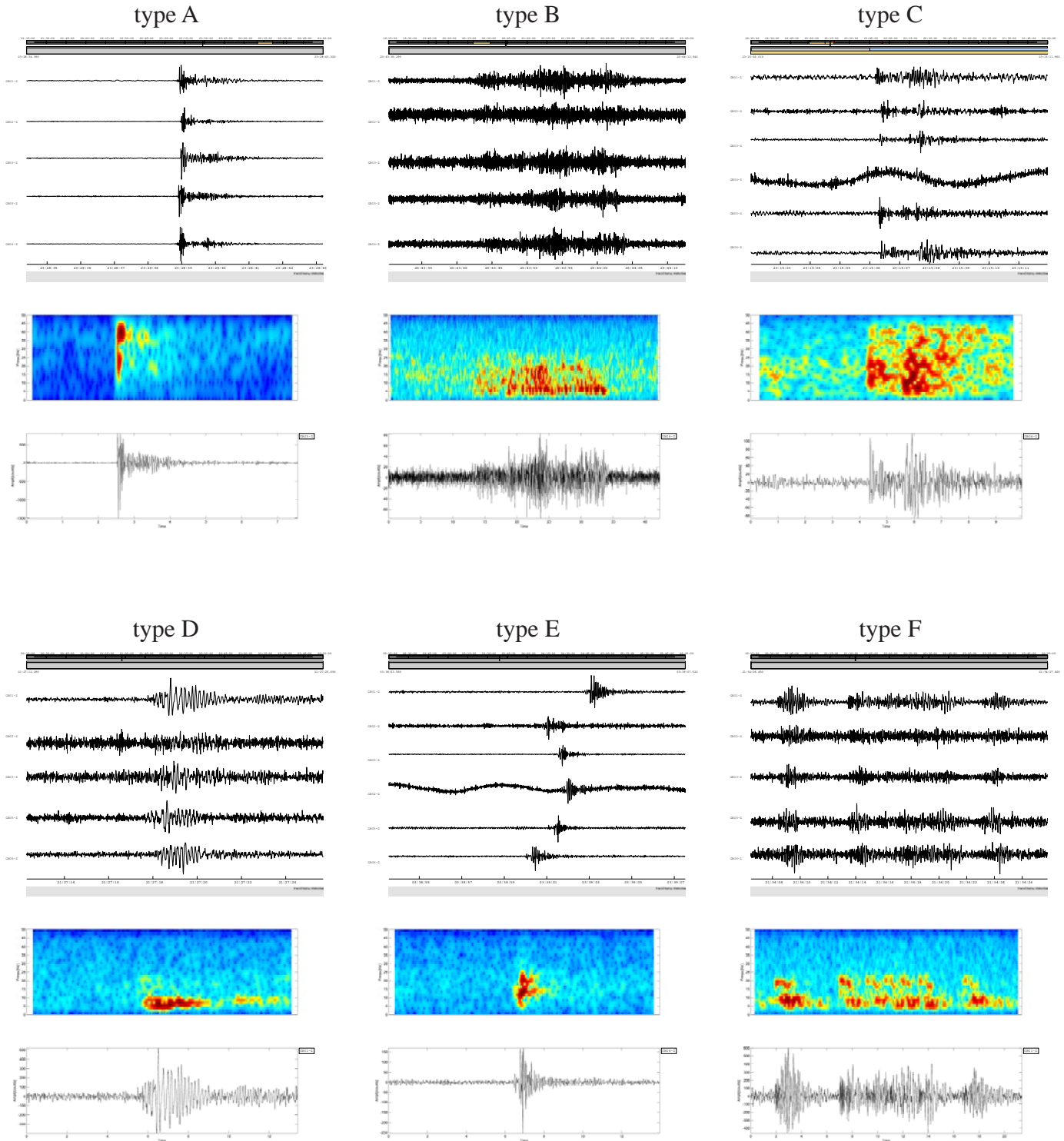


Figure 8: Example seismograms and spectrograms for event types A, B, C, D, E and F. Event type Z can't be represented by one example because this event type holds all candidates which can't be assigned to a certain event type.

## 5.2 Event localization

For events with sufficient signal-to-noise ratio and a clear first break of the P-wave, localization is done using first-arrival times and existing P-wave velocity models. The localization is done with the software NLLoc. This software calculates the travel times by solving the eikonal equation (Podvin and Lecomte, 1991) and grid-search and probabilistic methods are used for finding the hypocenter (Lomax *et al.*, 2000, Lomax *et al.*, 2001).

The method has been successfully tested using controlled seismic sources (dynamite shots). An example, how the localization performs on different seismic events is given in Figure 9. The event epicentre is well defined, but the resolution with depth allows no determination of the event's hypocentre.

## 6 Results

### 6.1 Overview

The results of the monitoring networks located at Gradenbach and Steinlehen are presented. The short-time monitoring networks installed at Hochmais/Atemskopf and Niedergallmigg/Matekopf yielded to an overview of the possible seismic activity of the mass-movements and, most important, helped to develop the design of an all-season working monitoring network. Some events have been found which show a similarity to events recorded at other mass-movements, but, because of the early stage of the research project, more detailed conclusions couldn't be made at that time.

A reprocessing of the data recorded at Hochmais/Atemskopf and Niedergallmigg/Matekopf, especially NG200606, with the newly gained insights on micro-earthquakes will be of value and should be a task in the ISDR20 successor project "Monitoring and Predicting Acceleration and Deceleration of Large Landslides".

### 6.2 Gradenbach

Up to now, continuous data of more than one year recorded between 02.2007 and 04.2008 at the permanent monitoring network Gradenbach has been processed. The events have been automatically detected and classified by a human operator. To prevent misinterpretations of man-made signals, only data recorded during night-time (20:00 to 8:00) has been taken into account.

The monthly recorded amount of the candidates of event types A, B, C and F is shown in Figure 10, a more detailed temporal distribution can be found in Appendix B. The four event types A, B, C and F are considered as being excited by the mass-movement. Events of type A, B and F tend to occur in clusters and most of the type F events are recorded only in December 2007 (see Appendix B, Figure 10).

The abrupt increase of seismic activity in December going along with the first occurrence of type F events since

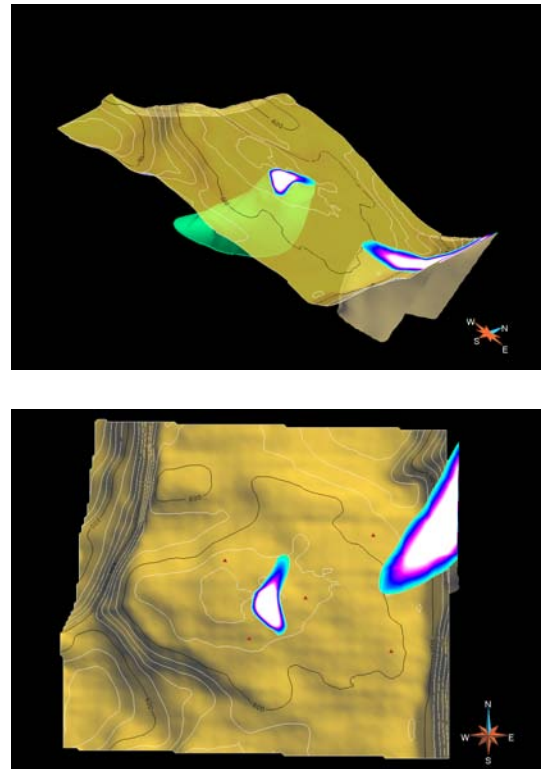


Figure 9: Example of localization of two different events recorded at HA. A 3D view (top) and a top view (bottom) are shown. The images show the topography of the area, the probability density function (surface plots) and the monitoring stations (red triangles). One event (a micro-earthquake) forms a clear minimum inside the monitoring network, the second event, a local earthquake, forms a channel-like shape, pointing into the direction of the earthquake's epicenter.

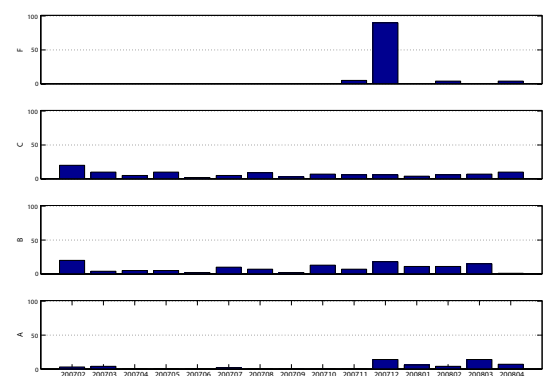


Figure 10: Monthly amount of classified candidates of type A, B, C and F.

the beginning of seismic monitoring at Gradenbach can be clearly seen. This change of seismic activity in December 2007 precedes an era of low seismic activity with a complete missing of type A events. The obvious variation of seismic activity and the isolated occurrence of type F events during a time period of only three weeks strengthens the idea of episodic creep of the mass-movement, which is a research topic of the ISDR20 successor project "Monitoring and Predicting Acceleration and Deceleration of Large Landslides".

### 6.2.1 Localization of type A events

Most of the type A events show a good p-wave onset. These events have been localized. Figure 11 shows the epicentre location of 15 type A events. The epicentres form two clusters, one in the lower part, and the other in the middle part of the mass-movement. The cluster in the lower part falls within a region of an over steepened slope where erosion events like small rock falls occur.

### 6.2.2 Type F events in period of high seismic activity

In December 2007 events of type F occur frequently for about 3 weeks. These events have not been recorded before and only a few of these events have been recorded after December 2007. The occurrence of type F events is characterized by forming temporal clusters lasting for about 30 minutes to 1 hour. The clusters consist of single events showing multiple high frequent onsets and a low frequent end (see Figure 12) or a sequence of these single events with the single events being separated by 1 to 2 seconds (Figure 13).

### 6.2.3 Coincidence of micro-earthquakes and a global earthquake

One type A event recorded during the high active period in December 2007 is of special interest. It occurs right after the p-wave onset of a global earthquake. The event happens 30 seconds after the P-wave onset of a mb=5.3 earthquake with the epicentre at the Aleutian islands (epidistance=81°). Figure 14 and Figure 15 show the seismogram and the spectrogram of the event.

A distinct localization of the event can't be done because of missing clear p-wave onset. A visual inspection of phases belonging together and the amplitude distribution indicates an epicentre in the upper part of the mass-movement.

Given this event and a similar event recorded at a different mass-movement (Steinlehen, see Figure 17), the possibility of triggering a micro-earthquake on the mass-movement by another large event should be considered in the future and will be task of the successor project.

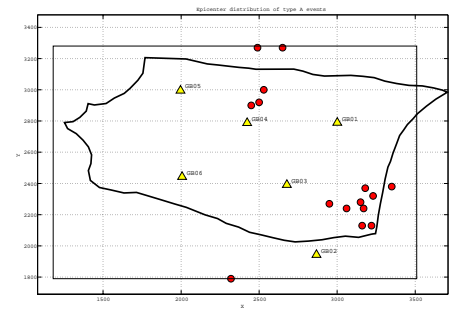


Figure 11: Epicenter plots of type A events. The stations (yellow triangles), the mass-movement boundary (thick black line), the border of the NLLoc search grid (black rectangle) and the epicentres (red circles) are shown. The epicentres cluster in two regions. Three of the events localize at the border of the search grid. This is most likely because of missing or poor time picks due to bad S/N ratio.

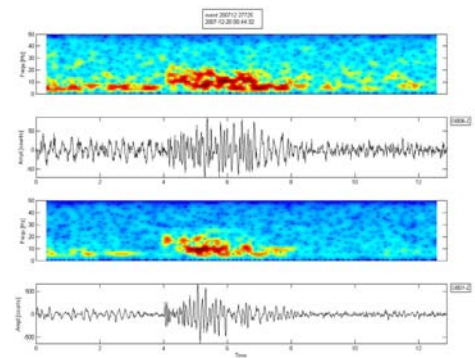


Figure 12: Seismogram and spectrogram of a type F event. This example shows a single event. Each single event consists of multiple high frequent parts followed by a low frequent end.

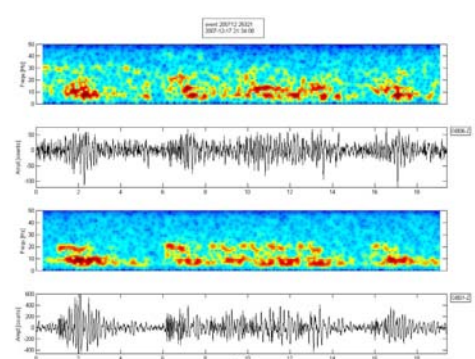


Figure 13: Seismogram and spectrogram of a type F event. This example shows the frequent succession of single type F events.

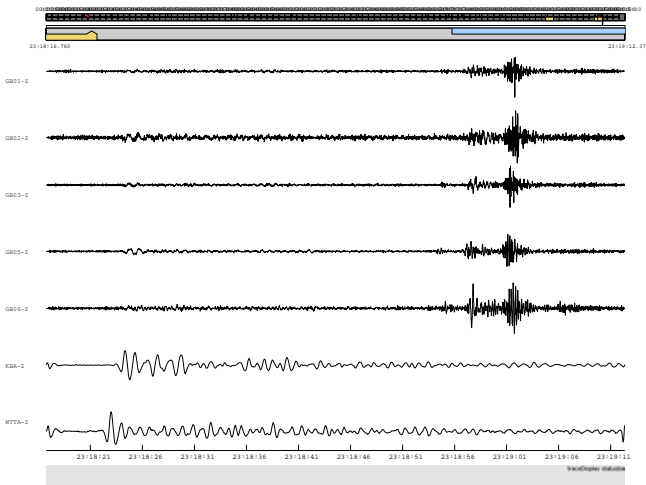


Figure 14: Seismogram of a micro-earthquake following the p-wave onset of a global earthquake. Stations KBA and WTTA are observatories nearby the mass-movement (KBA: 35 km, WTTA: 100 km).

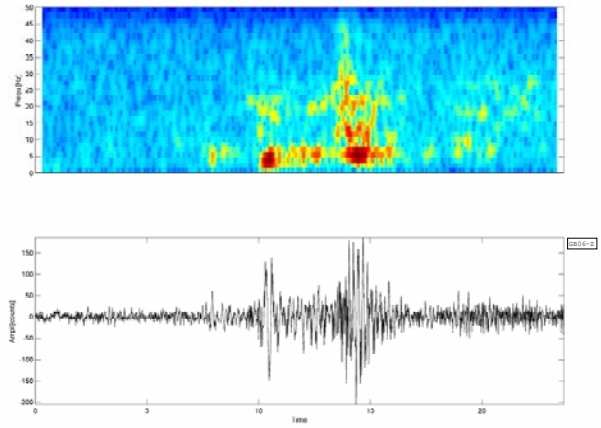


Figure 15: Spectrogram of a micro-earthquake following the p-wave onset of a global earthquake.

### 6.3 Steinlehn rock slide

The monitoring project at Steinlehn has been accomplished in cooperation with alpS - Centre of Natural Hazard Management. To reduce the influence of man-made seismic noise, only the night-time from 20:00 to 7:00 local time of the monitoring network SL200707 has been taken into account. 130 Events have been classified as candidates.

Because of a missing P-wave velocity model which prevents exact epicentre locations, an estimation of the event location has been made using the station distribution of event onsets and amplitude distributions. Several candidates are only present on stations inside the network (most of them recorded on stations SL05, SL08 and SL03 with the first onset on SL05) or are recorded only at the uppermost stations (SL01, SL02). These events are thought to be caused by the creep of the mass-movement.

According to these criteria, 27 events have been related to the mass-movement (MM-events) and based on the distribution of the stations with a recognizable event onset, the estimated event epicentres have been assigned to a region of the mass-movement: top part and active slab part. The top part describes a region around stations SL01 and SL2, the active slab part a region near SL05, SL08 and SL03. The 27 MM-events consist of three event types (A, B and F) where-at the majority of the MM-events are of type A and type B events. Figure 16 gives an overview of the occurrence of the MM-events.

Two of the MM-events are of special interest because they occur right after a global earthquake. The global earthquake is of magnitude  $m_b=6.1$  and its epicentre is located in western Brazil (epidistance= $91^\circ$ ). One event is recorded at SL05 20 seconds after the earthquake P-wave onset, a second one is recorded at SL05, SL08 and SL03 58 seconds after the P-wave onset of the same global earthquake. Figure 17 shows the seismograms of the global earthquake and the two subsequent MM-events. A detailed view of the second MM-event is shown in Figure 18 and the spectrogram of this MM-event recorded at station SL05 can be seen in Figure 19.

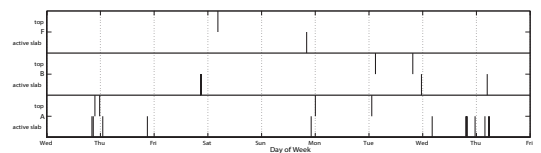


Figure 16: Temporal distribution of MM-events recorded at Steinlehn. Each vertical bar indicates one event. The MM-events are listed according to their estimated epicentre region (top- and active slab region).

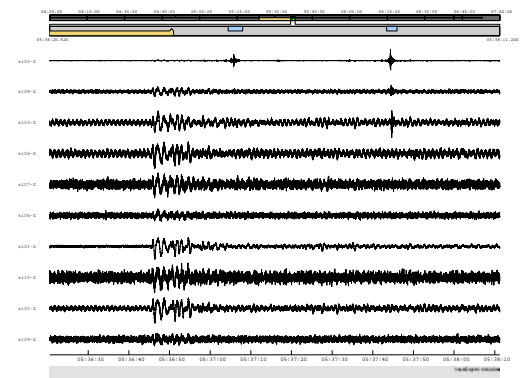


Figure 17: Seismogram of two micro-earthquakes following the p-wave onset of a global earthquake.

## 7 Discussion

The short-time monitoring projects and especially the permanent monitoring project at Gradenbach proved that the creep of deep-seated mass-movements is capable of inducing seismic events. It showed that new methods have to be developed to process the data recorded at the mass-movement and that standard seismological methods have to be adapted to work within small scale monitoring networks. Moreover the ISDR20 project revealed many open questions which have to be solved in ongoing research.

More than one year of permanent monitoring at Gradenbach exposed that it is essential to run the monitoring network all-season and not to focus on isolated time periods. Taking a look at December 2007, it can be seen, that even a measurement gap of only 3 weeks would have caused a missing of a completely new seismic event recorded at the mass-movement.

Seismic monitoring projects at other locations help to identify events induced by the movement of the slope. Although a second permanent monitoring network might be a financial challenge, at least regular short-time periods should be accomplished at a suitable mass-movement (e.g. Steinlehnen). This will broaden the standard of knowledge according to micro-seismic events and will improve the event identification. Also outstanding events (e.g. possible trigger mechanisms) can be more reliably evaluated if recorded on two different locations.

Three special events have been recorded. One at Gradenbach and two at Steinlehnen. The events occurred several 10<sup>th</sup> of seconds after the P-wave onset of a global earthquake. The waveform and the spectrogram of the special events show several similarities. Taken the rare occurrence of such kind of events and the fact that a similar event follows a global earthquake at two different locations makes it quite doubtful to simply account pure coincidence for this occasion. The possibility of mass-movement events being triggered by other seismic events should be taken into account and included in the ongoing research.

The temporal restricted occurrence of type F events in December 2007 strengthens the idea of episodic creep of the mass-movement. This is a major research part in the successor project "Monitoring and Predicting Acceleration and Deceleration of Large Landslides" and given the data recorded during ISDR20 we have got an excellent background to start with.

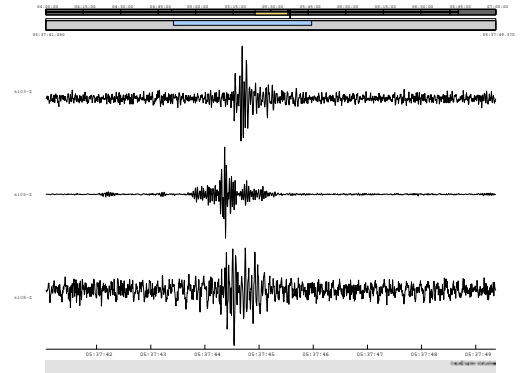


Figure 18: Detailed view of the second micro-earthquake.

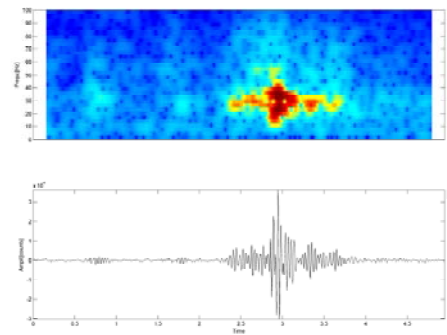


Figure 19: Spectrogram of the second micro-earthquake.

## 8 References

- Brückl, E. & Mertl, S., 2006. Seismic Monitoring of Deep-Seated Mass Movements. in *Proceedings of INTERPRAEVENT International Symposium "Disaster Mitigation of Debris Flows, Slope Failures and Landslides."* pp. 571-580 Universal Academy Press, Inc. / Tokyo, Japan.
- Gonzalez, R.C. & Woods, R.E., 2002. *Digital image processing*, second edition edn, Vol., pp. Pages, Prentice Hall.
- Hart, D.M., Merchant, B.J., Harris, J.M. & Young, C.J., 2005. The 2005 Matseis and NNSA seismic regional analysis tools. in *27th Seismic Research Review*.
- Havskov, J. & Ottemöller, L., 1999. Electronic Seismologist: SeisAn Earthquake Analysis Software, *Seismological Reserach Letters*, 70, 532 - 535.
- Joswig, M., 1990. Pattern recognition for earthquake detection, *Bulletin of the Seismological Society of America*, 80, 170-186.
- Joswig, M., 1994. Knowledge-based seismogram processing by mental images, *IEEE*, 24, 429-439.
- Lomax, A., Virieux, J., Voant, P. & Berge, C., 2000. Probabilistic earthquake location in 3D and layered models: Introduction of a Metropolis-Gibbs method and comparison with linear locations. in *Advances in Seismic Event location*, eds Thurber, C. H. & Rabinowitz, N. Kluwer Academic Publishers.
- Lomax, A., Zollo, A., Capuano, P. & Virieux, J., 2001. Precise, absolute earthquake location under Somma&#x2013;Vesuvius volcano using a new three-dimensional velocity model, *Geophysical Journal International*, 146, 313-331.
- Mehnert, A. & Jackway, P., 1997. An improved seeded region growing algorithm, *Pattern Recognition Letters*, 18, 1065-1071.
- Mertl, S. & Brückl, E., 2007. Observation of fracture processes in creeping rock masses by seismic monitoring, *Proceedings of 11th congress of the international society for rock mechanics, Lisbon, Portugal 9-13 July 2007*.
- Podvin, P. & Lecomte, I., 1991. Finite difference computation of traveltimes in very contrasted velocity models: a massively parallel approach and its associated tools, *Geophysical Journal International*, 105, 271-284.
- Zangerl, C., Eberhardt, E., Schönlaub, H. & Anegg, J., 2007. Deformation behavior of deep-seated rockslides in crystalline rock. in *Rock Mechanics: Meeting Society's Challenges and Demands*, eds Eberhardt, Stead & Morrison. Tylor & Francis Group, London.

## Appendix

### A. Seismon – Data handling and processing Software

#### A.1. Overview

Seismon is an interactive program for seismological data analysis. The main focus lies in processing of continuous small scale monitoring network data. Seismon is developed with Matlab® and provided under the Gnu General Public License. The focus of the Seismon project is to provide a complete seismological data analysis software written in a wide spread and easy to understand programming language. This software should support low budget scientific projects in managing and processing their data and provides an easy to use interface to develop new algorithms and easily test them on real-world data.

Seismon is based on a modular approach. That means, by following a few interface design rules new code can be integrated into Seismon without changing the source code of the main program. Each additional functionality is provided to Seismon as a **package**. The current version of Seismon requires Matlab® version R2008a and extensively uses the enhanced object oriented programming approach of this Matlab® version. As a database backend, the MySQL server version 5.1 is used. The Seismon main window is shown in Figure 20.

A Seismon workflow consists of 4 major steps:

- raw data conversion
- data import
- continuous data processing
- event based data processing

#### A.2. Raw data conversion

The conversion of raw data from different seismic recording equipment is supported including RefTek Texan and Reftek 130. The raw data conversion routines mainly call the conversion programs provided by the manufacturer. Seismon facilitates the usage of these conversion programs by providing a graphical frontend and storing parameters used for the conversion (see Figure 21 for an example).

#### A.3. Data import

Within Seismon, the data is stored in a binary Matlab format. Seismon supports the import of several standard seismic data formats. The idea behind supporting as many data formats as possible is the problem of low-budget projects being forced to use different recording systems within one project. Usually each recording system is based on a different data format and finding an up-to-date and working data

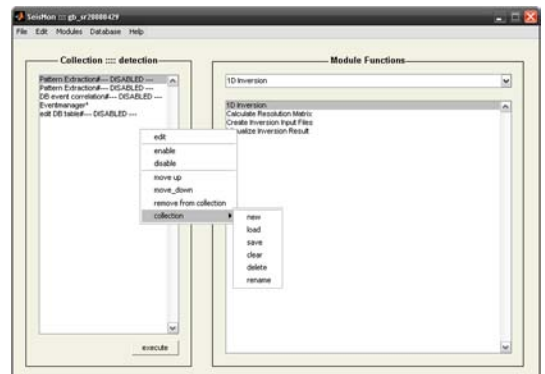


Figure 20: Seismon main window providing the collection management and the module functions.

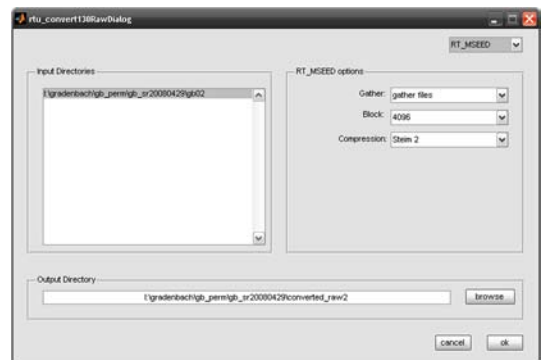


Figure 21: Reftek 130 raw data conversion frontend.

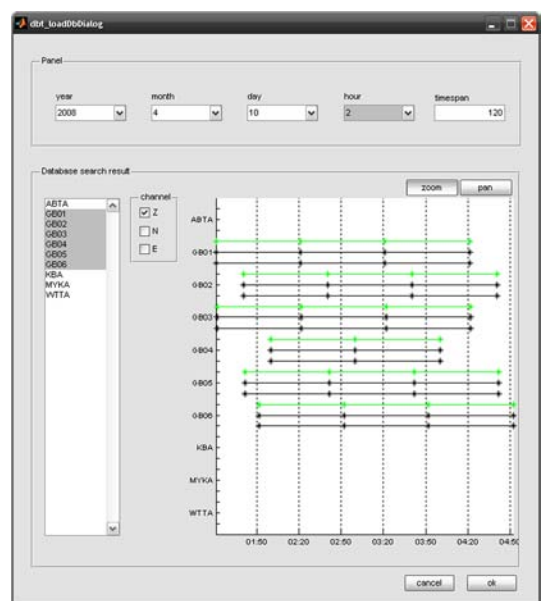


Figure 22: Database trace selection dialog.

conversion program is not an easy task. The Seismon import functions are either based on tested open source libraries or the import code is directly implemented in Matlab®. This gives the user a better control over the data handling and possible errors in the data are easier to detect.

Data formats supported so far are:

- miniSeed
- Reftek SEGy (RSY)
- GSE 2.1 (cm6 compressed)
- Standard SEGy
- Guralp Compressed Fileformat (gcf)
- SAC
- PDAS

#### A.4. Continuous data processing

The processing of continuous data is a major part of the Seismon software. This step includes visualization of seismic data supporting different sampling rates and data gaps, and automated event detection. The event detection algorithm presented in this report is implemented as a Seismon package.

Major tools in continuous data processing are:

- Load data from database (Figure 22)
- Data visualization (providing processing tools like frequency filtering, time-frequency analysis, time- and amplitude picking) (Figure 23)
- Automated event detection

#### A.5. Event based data processing

Automatic or manually defined events are stored in a database. The Seismon event manager (see Figure 24) provides a tool to easily access and visualize the event data. Further data processing is based on the defined events and include export to standard seismic data formats or event localization using NLLoc.

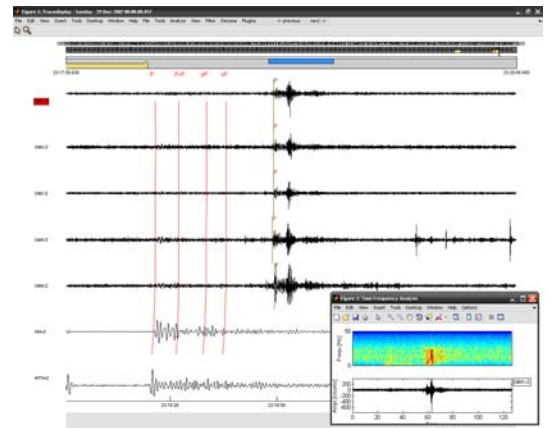


Figure 23: Trace display window with time picks, AK135 traveltimes overlay and spectrogram plot of a selected trace. The events stored in the database are shown in the gray overview bars at the top.

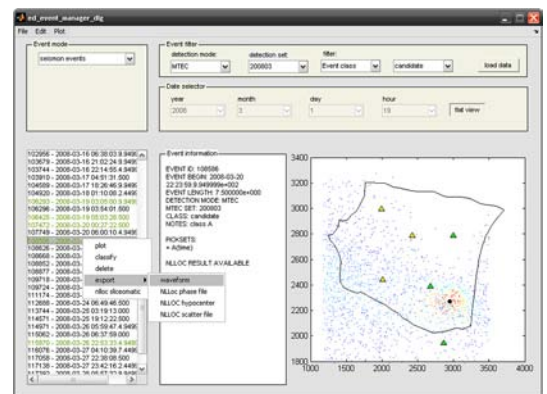


Figure 24: Event manager dialog window. The eventlist, event details of a selected events and the NLLoc pdf result is displayed.

## B. Temporal distribution of events

